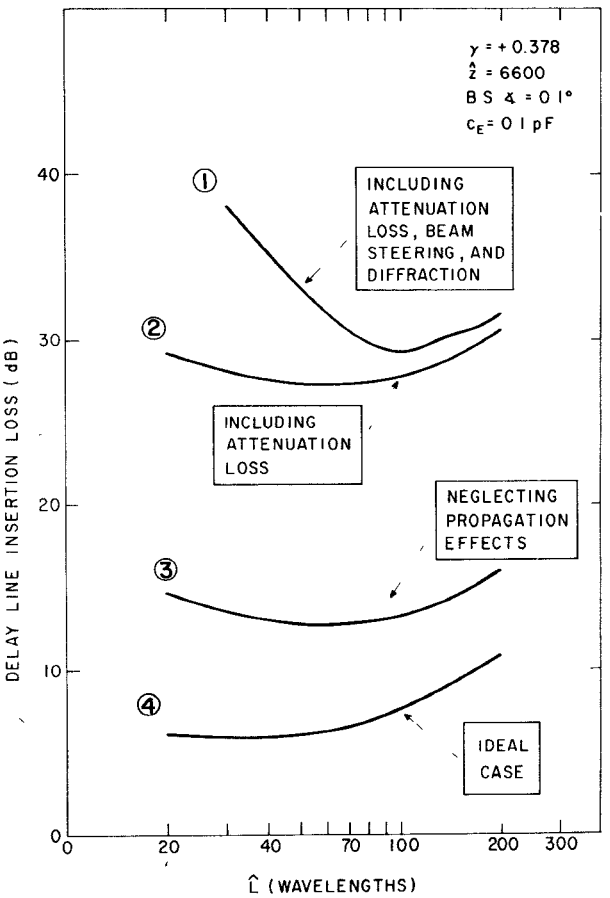

Fig. 9. Delay line insertion loss versus acoustic aperture curves used to choose optimum (minimum insertion loss) acoustic aperture Curve 1 includes real transducer effects ($Q = 30$, $\rho/t = 0.345\ \Omega/\square$, and $C_E = 0.1$ pF). attenuation loss. beam steering. and diffraction. Curve 2 includes real transducer effects and attenuation loss. Curve 3 includes real transducer effects and attenuation loss. Curve 3 includes only transducer effects. Curve 4 is the ideal case corresponding to $Q = \infty$, $\rho/t = 0$, and $C_E = 0$ with zero propagation, beam steering and diffraction losses.

to the original Stanford design procedure [10], [11] is also presented in Fig. 9 for comparison. Here, $R_L = 0$, $R_G = 0$, $C_e = 0$, BS $\not\propto = 0$, and attenuation and diffraction losses are neglected. The substantial difference is easily seen.

IV. CONCLUSIONS

Typical sets of design curves for combined beam steering and diffraction losses have been presented. These curves are expected to be particularly useful in aiding in the choice of material for any given application and in alerting the surface wave engineer as to when beam steering and diffraction become serious design constraints.

It has been shown that in the presence of beam steering, each material presents a special case and universal combined curves are not possible.

The standard design optimization procedures for determining interdigital transducer finger overlap have been extended to include beam steering and diffraction losses in addition to finger loss and external circuit effects.

REFERENCES

[1] J. J. Campbell and W. R. Jones, "A method for estimating optimal crystal cuts and propagation directions for excitation of piezoelectric surface waves," *IEEE Trans. Sonics Ultrason.*, vol. SU-15, pp. 209–217, Oct. 1968.
[2] M. B. Schulz, B. J. Matsinger, and M. G. Holland, "Temperature dependence of surface wave velocity on α-quartz," *J. Appl. Phys.*, vol. 41, pp. 2755–2765, June 1970.
[3] M. B. Schulz and M. G. Holland, "Temperature dependence of surface acoustic wave velocity in lithium tantalate," *IEEE Trans. Sonics Ultrason.*, vol. SU-19, pp. 381–384, July 1972.
[4] A. J. Slobodnik, Jr., P. H. Carr, and A. J. Budreau, "Microwave frequency acoustic surface-wave loss mechanisms on $LiNbO_3$," *J. Appl. Phys.*, vol. 41, pp. 4380–4387, Oct. 1970.
[5] A. J. Budreau and P. H. Carr, "Temperature dependence of the attenuation of microwave frequency elastic surface waves in quartz," *J. Appl. Phys.*, vol. 18, pp. 239–241, Mar. 1971.
[6] A. J. Slobodnik, Jr., and A. J. Budreau, "Acoustic surface wave loss mechanisms on $Bi_{12}GeO_{20}$ at microwave frequencies," *J. Appl. Phys.*, vol. 43, pp. 3278–3283, Aug. 1972.
[7] A. J. Slobodnik, Jr., and E. D. Conway, "The effect of beam steering on the design of microwave acoustic surface wave devices," in *Int. Microwave Symp. Dig.*, May 1970, pp. 314–318.
[8] T. L. Szabo and A. J. Slobodnik, Jr., "The effect of diffraction on the design of acoustic surface wave devices," *IEEE Trans. Sonics Ultrason.*, vol. SU-20, pp. 240–251, July 1973.
[9] I. M. Mason and E. A. Ash, "Acoustic surface-wave beam diffraction on anisotropic substates," *J. Appl. Phys.*, vol. 42, pp. 5343–5351, Dec. 1971.
[10] W. R. Smith, H. M. Gerard, J. H. Collins, T. M. Reeder, and H. J. Shaw, "Analysis of interdigital surface wave transducers by use of an equivalent circuit model," *IEEE Trans. Microwave Theory Tech. (Special Issue on Microwave Acoustics)*, vol. MTT-17, pp. 856–864, Nov. 1969.
[11] ——, "Design of surface wave delay lines with interdigital transducers," *IEEE Trans. Microwave Theory Tech. (Special Issue on Microwave Acoustics)*, vol. MTT-17, pp. 865–783, Nov. 1969.
[12] D. B. Armstrong, "Research to develop microwave acoustic surface wave delay lines," Litton Industries, San Carlos, Calif., Final Rep. AFCRL-72-0378, June 1972.
[13] H. Gerard, M. Wauk, and R. Weglein, "Large time-bandwidth product microwave delay line," Hughes Aircraft Co., Fullerton, Calif., Tech. Rep. ECOM-03852, Oct. 1970.
[14] R. D. Weglein and E. D. Wolf, "The microwave realization of a simple surface wave filter function," in *Int. Microwave Symp. Dig.*, June 1973, pp. 120–122.
[15] A. J. Slobodnik, Jr., and T. L. Szabo, "Ultralow-diffraction acoustic-surface-wave propagation on $Bi_{12}GeO_{20}$," *Electron Lett.*, vol. 9, pp. 149–150, Mar. 1973.
[16] M. B. Schulz and J. H. Matsinger, "Rayleigh-wave electromechanical coupling constants," *Appl. Phys. Lett.*, vol. 20, pp. 367–369, May 1972.
[17] A. J. Slobodnik, Jr., "UHF and microwave frequency acoustic surface wave delay lines, I. Design." Air Force Cambridge Res. Lab., Bedford, Mass., 1973.
[18] G. W. Farnell, I. A. Cermak, P. Silvester, and S. K. Wong, "Capacitance and field distributions for interdigital surface-wave transducers," *IEEE Trans. Sonics Ultrason.*, vol. SU-17, pp. 188–195, July 1970.

Application of Microstrip Analysis to the Design of a Broad-Band Electrooptical Modulator

EIKICHI YAMASHITA, MEMBER, IEEE, KAZUHIKO ATSUKI, AND TOSHIHIKO AKAMATSU

***Abstract*—This short paper describes a proposed structure of a broad-band electrooptical modulator and an application of existing microstrip analysis programs to determine dimensions of the structure for a broad-band property. Results of numerical computations indicate that it is possible to obtain a broad-band modulator by using $LiNbO_3$ or $LiTaO_3$.**

I. INTRODUCTION

The impedance matching problem of a traveling-wave electrooptical modulator has not been solved for years, though it is an important factor in the limitation of the bandwidth of the modulator [1], [2]. Recently, a lithium tantalate traveling-wave modulator has been reported which has the characteristic impedance close to the normal 50-Ω impedance system [3]. A structural design consideration to match the light velocity and the modulation wave velocity has also been reported [4]. The satisfaction of only one of two conditions, the impedance matching and velocity matching, may not be enough to obtain a broad-band property. Perhaps, the best way is to search out a modulator structure by using a computer calculation so as to satisfy these two conditions simultaneously.

II. TRAVELING-WAVE ELECTROOPTICAL MODULATORS

One of the proposed modulator structures is shown in Fig. 1(a). Material 1 is a small electrooptical crystal to modulate laser light, material 2 and 3 dielectric, and material 4 conductor to guide

Manuscript received July 9, 1973; revised November 2, 1973. This work was supported in part by the Research Project on Laser Communications.
The authors are with the University of Electro-Communications, Chofu-shi, Tokyo, Japan.

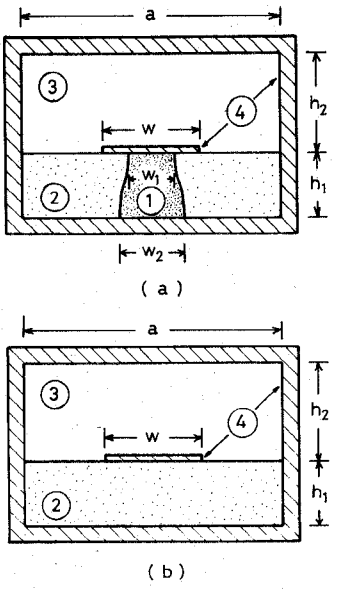

Fig. 1. (a) Modulator structure. (b) Microstrip structure after material 1 of the above structure (a) is replaced by material 2.

modulation waves. These form a strip transmission line of length L. Quasi-TEM waves can propagate along this line and the group velocity of this mode v_m is almost dispersionless up to high microwave frequencies. The refraction index of the electrooptical crystal is slightly changed when the modulation waves are applied to the crystal. This effect is accumulated while the laser beam advances through the crystal with the velocity v_l. When v_m is equal to v_l, the light and modulation waves are synchronized and the modulation bandwidth is not limited. When v_m is not equal to v_l, the modulation bandwidth is approximately given by [1]

$$0 < f_m < \frac{v_m}{4L \mid 1 - v_m/v_l \mid} \tag{1}$$

where f_m is the modulation frequency.

Since the laser beam is very narrow, v_l is determined only by the optical characteristics of the crystal and independent of line configurations. v_m can be adjusted to v_l by a suitable choice of materials and dimensions of the modulator if an analysis program already exists.

Another factor in the limitation of the modulator bandwidth is the mismatching of the transmission line to the outside circuit, say a 50-Ω coaxial cable system. When the characteristic impedance of the transmission line Z_m is not equal to the outside circuit impedance Z_c, standing waves appear in the modulator and a simple analysis gives the bandwidth due to the standing waves as

$$0 < f_m < \frac{v_m}{4L}. \tag{2}$$

After all, the cross-sectional structure of an electrooptical modulator has to be chosen so as to satisfy simultaneous matching conditions

$$Z_m = Z_c \qquad \text{and} \qquad v_m = v_l. \tag{3}$$

III. A PROPOSED MODULATOR STRUCTURE

Fig. 1(a) shows a proposed modulator structure to satisfy the simultaneous matching condition (3). The boundary surfaces between materials 1 and 2 are formed along the electric line of force which is almost linear. We apply the existing microstrip analysis program of the structure as shown in Fig. 1(b) [5]–[7] to the above modulator structure.

Suppose material 1 is replaced by material 2 in Fig. 1(a). Then the structure is reduced to the microstrip line as shown in Fig. 1(b). Since the distribution of the electric line of force is not affected by by this replacement, the analytical knowledge of the electric line of force in Fig. 1(b) can be directly applied to the analysis of the modulator. Though the electric charge density on the boundary between the strip and material 1 is changed by the replacement, the amount of the change can be calculated by knowing the dielectric constant in each material and applying Gauss's theorem. After all, a formula for the line capacitance C of the modulator is derived and from which the line capacitance C_0 for the case of $\epsilon_1^* = \epsilon_2^* = \epsilon_3^* = 1$ can be also obtained. Then, the characteristic impedance of the modulator line is given by

$$Z_m = \frac{1}{(CC_0)^{1/2} v_0} \tag{4}$$

and the modulation wave velocity is given by

$$v_m = \left(\frac{C_0}{C}\right)^{1/2} v_0 \tag{5}$$

where v_0 is the velocity of light in vacuum. From (3), C and C_0 have to satisfy the conditions

$$C_0 = \frac{v_l}{Z_c v_0^2} \tag{6}$$

$$C = \frac{1}{Z_c v_l}. \tag{7}$$

IV. NUMERICAL RESULTS

The result of computer search indicates that it is possible to satisfy the simultaneous matching condition by a suitable choice of the crystal width as shown in Table I and Fig. 2.

The starting position and arriving position of the electric line of force can be calculated by examining the charge density distribution based on the microstrip analysis. The relation between W_2/h_1 and W_1/h_1 thus calculated is shown in Fig. 3 for the case of $LiNbO_3$ by a solid line and of $LiTaO_3$ by a dotted line. Though the boundary surfaces of the crystal are to be shaped along the electric line of force, these surfaces could be approximated by a straight line. Since the laser beam does not pass the surface, this line is not necessarily optically straight.

When the impedance matching and the velocity matching are

TABLE I
DIMENSIONS OF THE MODULATOR TO SATISFY THE TWO MATCHING CONDITIONS

	case 1	case 2
Electro-optical Crystal	$LiNbO_3$	$LiTaO_3$
ϵ_1^*	28	43
ϵ_2^* (Teflon)	2.1	2.1
ϵ_3^* (Air)	1.0	1.0
$n = V_0/V_l$	2.284	2.176
$Z_m = Z_c$ (ohms)	50	50
a/h_1	3.35	3.35
h_2/h_1	2.0	2.0
w/h_1	0.9	1.0
w_1/h_1	0.35	0.21

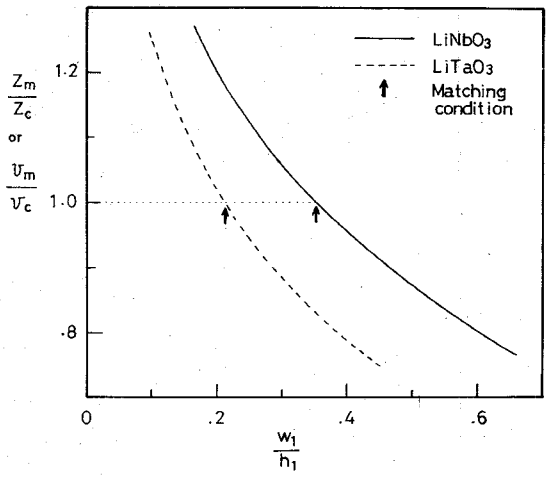

Fig. 2. Numerical results to indicate dimensions to satisfy the two matching conditions for the case of $LiNbO_3$ and $LiTaO_3$ crystal.

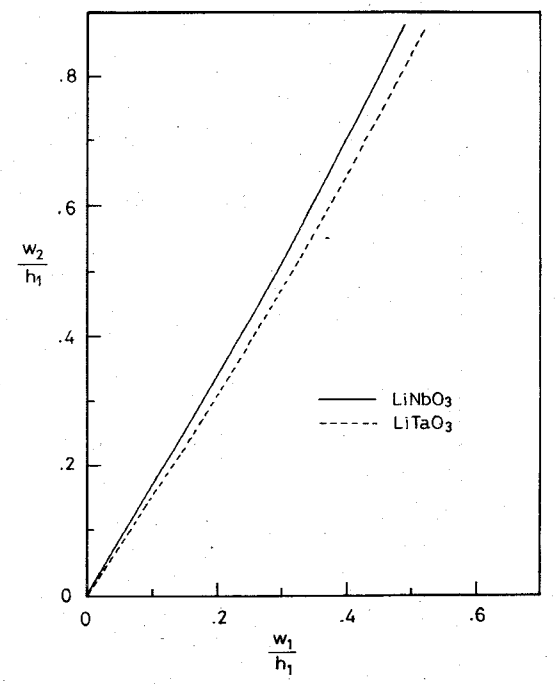

Fig. 3. Relation between the two widths W_1 and W_2 for the case of $LiNbO_3$ and $LiTaO_3$ crystal.

thus achieved, the final bandwidth of a modulator using a quasi-TEM line is limited by the dispersion characteristics at high microwave frequencies.

Note Added in Proof: The length and the transverse dimension of traveling-wave modulators will eventually be limited by the diffraction effect of the laser beam [1], [2]. This limitation is also important in order to achieve the modulation with minimum power/bandwidth.

ACKNOWLEDGMENT

The authors wish to thank Prof. T. Okabe for his helpful advice and E. Kiuchi for his assistance.

REFERENCES

[1] I. P. Kaminow and E. H. Turner, "Electrooptical light modulators," *Proc. IEEE (Special Joint Issue on Optical Electronics with Applied Optics)*, vol. 54, pp. 1374–1390, Oct. 1966.
[2] F.-S. Chen, "Modulators for optical communications," *Proc. IEEE (Special Issue on Optical Communications)*, vol. 58, pp. 1440–1457, Oct. 1970.
[3] G. White, "A one-gigabit-per-second optical PCM communications system," *Proc. IEEE* (Lett.), vol. 58, pp. 1779–1780, Oct. 1970.
[4] E. Yamashita and K. Atsuki, "A proposed microwave structure and design method for traveling-wave modulation of light," *IEEE Trans. Microwave Theory Tech.* (Corresp.), vol. MTT-17, pp. 118–119, Feb. 1969.
[5] ——, "Analysis of thick-strip transmission lines," *IEEE Trans. Microwave Theory Tech.* (Corresp.), vol. MTT-19, pp. 120–122, Jan. 1971.
[6] ——, "Analytical method for transmission lines with thick-strip conductor, multi-dielectric layers, and shielding conductor," *J. Inst. Electron. Commun. Eng. Jap.*, vol. 53-b, pp. 322-328, June 1970.
[7] ——, "Strip line with rectangular outer conductor and three dielectric layers," *IEEE Trans. Microwave Theory Tech.*, vol. MTT-18, pp. 238–244, May 1970.

A MIC Phase-Locked Loop Avalanche Oscillator in X Band

J. SALMON

***Abstract*—This short paper describes the design and performances of a MIC phase-locked loop X-band avalanche oscillator. The output power (500 mW/CW), the input reference level (1 mW), the locking time (80 ns), and the simplicity of digital phase control makes it very attractive as a primary element of an active phased array.**

INTRODUCTION

Solid-state active phased arrays have always appeared attractive in radar applications. First, because the inherent losses of the passive phased array (more than 3 dB on signal at high microwave frequencies) are avoided, and second because these arrays are probably the best way to realize a powerful solid-state transmitter. However, these arrays can be expected to achieve industrial applications in radar only if the structure of each element is not too sophisticated.

Two approaches to solid-state arrays were considered until now. In the first approach, phase shifting and amplification were achieved at a lower frequency (S band, for instance, in the MERA [1]) and a high-power multiplier provided the right frequency. In the second approach phase shift and amplification were directly achieved at the right frequency. In both cases, phase shifting was made by quantified microwave phase shifters at low level, and amplification was made either by transistor or diode amplifiers (multistage). Altogether, that makes a great number of microwave (expensive) components.

The phase-locked loop (PLL) oscillator seems to be an economical way to realize high microwave gain, especially in X band and above. In addition, quantified phase control can be achieved easily by commutation at video frequencies instead of microwave phase shifters. The study presented below is the first step in the realization of an active element of an X-band phased array.

THEORETICAL BACKGROUND

The PLL principle is shown in Fig. 1 [2]. A portion of the signal provided by the voltage controlled oscillator (VCO) on one side and the reference on the other side enters a phase detector (PD). The output signal of that PD is sent through the baseband amplifier to the frequency control (varactor) of the VCO.

For a PLL, frequency synchronism is achieved throughout a band B when we have the following:

B G_oKS.
G_o Baseband amplifier (BBA) gain.
K Characteristic slope of the PD (V/rad).
S VCO's control characteristic (MHz/V).

For the system under study, the technical requirements were: minimum synchronization bandwidth $B = 30$ MHz; reference signal power: 1 mW (which leads to a PD characteristic K of 0.3 V/rad

Manuscript received May 14, 1973; revised August 2, 1973. This work was supported by the Service Technique des Télécommunications de l'Air under Contract 70/86 050
The author is with Thomson—CSF, Malakoff, France.